

The hidden negative differential thermal conductance

Zi-chen Zhang, Zheng Liu, and Chang-shui Yu^{1,*}

¹*School of Physics, Dalian University of Technology, Dalian 116024, P.R. China*

(Dated: September 5, 2025)

Negative differential thermal conductance (NDTC), a hallmark of nonlinear quantum thermal transport, plays a critical role in the design of quantum thermal devices such as thermal diodes and transistors. The Lindblad dynamics predicts that the heat current through two coupled atoms increases with the increasing temperature difference of two bosonic reservoirs. However, in this paper, we uncover the suppressive effect on the heat current in this nonequilibrium system using the Bloch-Redfield master equations, which indicate the emergence of NDTC. Our findings underscore the crucial role of beyond-Lindblad dynamics in accurately capturing nonlinear features in quantum thermodynamic systems.

I. INTRODUCTION

Quantum thermodynamics provides the foundational framework for understanding energy conversion processes at the microscopic scale, where quantum coherence, entanglement, or other quantum phenomena may play a significant role. This theoretical framework, elucidating the interconversion of work and heat in quantum systems, forms the basis for quantum thermal devices, such as quantum engines [1–10], quantum refrigerators [11–17], and work extraction using quantum measurements [18–22], which demonstrates how quantum resources can be harnessed to control energy flows at the quantum level. Essentially, describing such systems requires a careful treatment of heat currents in open quantum systems, especially when they are driven far from equilibrium by temperature gradients between reservoirs. The Lindblad master equation, based on the Born-Markovian approximation and the secular approximation (ME), has been widely adopted for its simplicity and complete positivity in its ability to describe the dynamics of open quantum systems effectively [23–30], especially including quantum optics [31, 32], nuclear magnetic resonance [33], quantum transport [34] and chemical dynamical systems [35] attesting to the versatility in describing system-environment interactions [36–39].

The Lindblad ME is typically valid for weak system-bath coupling and large energy separations. Still, it fails in systems with small energy gaps, where coherence-mediated processes and non-secular energy exchange become significant. In contrast, the Bloch-Redfield (BR) master equation [32, 40–47] derived from second-order perturbation theory provides a more complete and accurate description of dissipative processes by retaining non-secular terms [41–43]. In particular, the BR master equation's steady-state solution corresponds to the mean force Gibbs (MFG) state [47–50], which properly incorporates system-environment coupling effects through a consistent perturbative expansion. The MFG state of

the BR master equation contains the second-order corrections in the system-environment coupling that modify both populations and coherences. In contrast, the Lindblad solution retains only the zeroth-order Gibbs distribution.

In this paper, we study the negative differential thermal conductance (NDTC)—a counterintuitive phenomenon in which increasing the temperature difference between thermal reservoirs leads to a decrease in the steady state heat current [51–54]. NDTC is not only of fundamental interest in nonequilibrium quantum thermodynamics but also a key enabler for functional microscopic thermal devices, such as quantum thermal diodes and transistors [55–61]. Our system is composed of two coupled atoms interacting with nonequilibrium thermal reservoirs [62–72]. Through perturbative analysis, we derive the BR master equation with the zeroth-order term recovering the Lindblad steady state, while second-order corrections reflect equilibrium features consistent with the MFG state. We uncover a suppressive effect on heat current arising from non-secular terms, which gives rise to NDTC in specific parameter regimes, even though the Lindblad dynamics predicts an increasing heat current with the temperature difference. The Redfield approach proves particularly powerful for describing nonequilibrium steady states and heat transport, providing crucial insights into the bridge between physically accurate dynamics and Markovian approximations for optimized quantum thermal control. This paper is organized as follows. In Sec. II, we give a brief description of our model and derive the master equations under the Born-Markov approximation. In Sec. III, we focus on calculating the steady states. In Sec. IV, we compare the heat currents derived from Lindblad and BR master equations. We conclude with a summary in Sec. V.

II. THE NONEQUILIBRIUM OPEN SYSTEM

Our system consists of two coupled two-level atoms (TLAs) interacting with a distinct thermal reservoir, respectively, as shown in Fig. 1. The Hamiltonian of the

* Electronic address: ycs@dlut.edu.cn

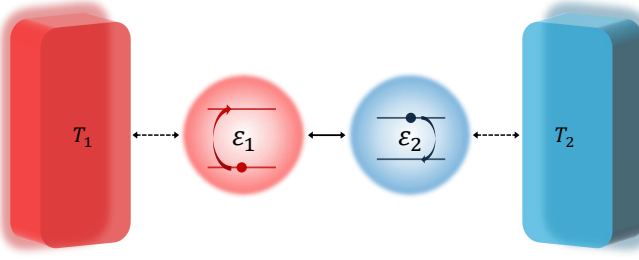


FIG. 1. The schematic illustration of our model, where the dashed line represents weak coupling, and the solid line represents strong coupling. The temperatures of two heat reservoirs are T_1 and T_2 , the energy separation of two qubits are ε_1 and ε_2 .

TLAs system reads

$$H_S = \frac{\varepsilon_1}{2} \sigma_1^z + \frac{\varepsilon_2}{2} \sigma_2^z + g \sigma_1^x \sigma_2^x, \quad (1)$$

where σ_i^z and σ_i^x are the Pauli matrices, and g is the coupling strength of two qubits, and we have set the Planck constant $\hbar = 1$ and the Boltzmann constant $k_B = 1$. Without loss of generality, let $\varepsilon_1 \geq \varepsilon_2$, then we have the eigenvalues of H_S as $s_1 = \beta, s_4 = -\beta, s_2 = \alpha, s_3 = -\alpha$, where

$$\alpha = \sqrt{\frac{(\varepsilon_1 - \varepsilon_2)^2}{4} + g^2}, \beta = \sqrt{\frac{(\varepsilon_1 + \varepsilon_2)^2}{4} + g^2}. \quad (2)$$

The corresponding eigenstates are

$$\begin{aligned} |s_1\rangle &= \sin \frac{\varphi}{2} |0,0\rangle + \cos \frac{\varphi}{2} |1,1\rangle, \\ |s_4\rangle &= \cos \frac{\varphi}{2} |0,0\rangle - \sin \frac{\varphi}{2} |1,1\rangle, \\ |s_2\rangle &= \cos \frac{\theta}{2} |1,0\rangle + \sin \frac{\theta}{2} |0,1\rangle, \\ |s_3\rangle &= -\sin \frac{\theta}{2} |1,0\rangle + \cos \frac{\theta}{2} |0,1\rangle, \end{aligned}$$

with

$$\tan \varphi = \frac{2g}{\varepsilon_1 + \varepsilon_2}, \tan \theta = \frac{2g}{\varepsilon_1 - \varepsilon_2}. \quad (3)$$

Suppose that the two heat reservoirs are always in the thermal state with inverse temperature $\beta_j = 1/T_j$, then the Hamiltonian of the reservoirs are

$$H_{Bj} = \sum_n \omega_{n,j} b_{j,n}^\dagger b_{j,n}, \quad (4)$$

where the summation is for all the harmonic oscillator modes of the j th reservoir. The interaction between the system and the reservoir is given by

$$H_{SBj} = \lambda_j B_j^x \sigma_j^x = \lambda_j B_j^x \sum_\mu V_j(\omega_\mu), \quad (5)$$

where λ_j is a dimensionless coupling constant that characterizes the strength of the interaction between the j -th atom and the j -th reservoir, $B_j^x = \sum_n \kappa_{j,n} (b_{j,n} + b_{j,n}^\dagger)$ and $\sigma_j^x = \sum_\mu V_j(\omega_\mu)$. Here $V_j(\omega_\mu)$ denote the eigenoperators satisfying $[H_S, V_j(\omega_\mu)] = -\omega_\mu V_j(\omega_\mu)$ [23, 26], given as

$$\begin{aligned} V_1(\omega_1) &= \sin \phi_+ (|s_2\rangle \langle s_1| - |s_4\rangle \langle s_3|), \\ V_1(\omega_2) &= \cos \phi_- (|s_4\rangle \langle s_2| + |s_3\rangle \langle s_1|), \\ V_2(\omega_1) &= \cos \phi_- (|s_2\rangle \langle s_1| + |s_4\rangle \langle s_3|), \\ V_2(\omega_2) &= \sin \phi_+ (|s_4\rangle \langle s_2| - |s_3\rangle \langle s_1|), \end{aligned}$$

with

$$\phi_+ = \frac{\theta + \varphi}{2}, \phi_- = \frac{\theta - \varphi}{2}, \omega_1 = \beta - \alpha, \omega_2 = \beta + \alpha, \quad (6)$$

and the index number $\mu \in \{1, -1, 2, -2\}$, noting that the negative frequency operator is given by $V_j(\omega_{-\mu}) = V_j(-\omega_\mu) = V_j^\dagger(\omega_\mu)$.

Thus, we can write the total Hamiltonian of the system and the reservoirs as

$$H = H_S + H_{B1} + H_{B2} + H_{SB1} + H_{SB2}. \quad (7)$$

Following the standard process [23, 26] in the framework of Born-Markov approximation, one can directly get the BR master equation governing the evolution of the system as

$$\frac{d\rho}{dt} = -i[H_S + H_{LS}, \rho] + \mathcal{L}_1(\rho) + \mathcal{L}_2(\rho), \quad (8)$$

where ρ is the density matrix of the TLAs, H_{LS} is the energy correction, i.e., the Lamb shift

$$H_{LS} = \sum_j \sum_{\omega, \omega'} \xi_j(\omega, \omega') V_j^\dagger(\omega') V_j(\omega), \quad (9)$$

and $\mathcal{L}_j(\rho)$ are the dissipators given by

$$\begin{aligned} \mathcal{L}_j(\rho) &= \sum_{\omega, \omega'} \gamma_j(\omega, \omega') \\ &\times \left(V_j(\omega) \rho V_j^\dagger(\omega') - \frac{1}{2} \{ V_j^\dagger(\omega') V_j(\omega), \rho \} \right). \end{aligned} \quad (10)$$

The coefficients are defined as

$$\xi_j(\omega, \omega') = \lambda_j^2 \frac{\Gamma_j(\omega) - \Gamma_j^*(\omega')}{2i}, \quad (11)$$

$$\gamma_j(\omega, \omega') = \lambda_j^2 (\Gamma_j(\omega) + \Gamma_j^*(\omega')), \quad (12)$$

where $\Gamma_j(\omega) = \int_0^\infty ds e^{i\omega s} \langle B_j^x(s) B_j^x \rangle$ is the forward Fourier transform of the reservoir correlation function $\langle B_j^x(s) B_j^x \rangle$. One can write

$$\Gamma_j(\omega) \equiv G_j(\omega) + iS_j(\omega), \quad (13)$$

$$G_j(\omega) = J_j(\omega) (\bar{n}_j(\omega) + 1), \quad (14)$$

$$S_j(\omega) = \frac{1}{\pi} P.V. \int_0^\infty J_j(\omega') \left(\frac{\bar{n}_j(\omega') + 1}{\omega - \omega'} + \frac{\bar{n}_j(\omega')}{\omega + \omega'} \right) d\omega', \quad (15)$$

where the *P.V.* denotes the Cauchy principal value of the integral, $\bar{n}_j(\omega) = (\exp(\beta_j\omega) - 1)^{-1}$ are the average photon number, and

$$J_j(\omega) = \pi \sum_n |\kappa_{j,n}|^2 \delta(\omega - \omega_n) \quad (16)$$

are the spectral density of the heat reservoirs. A more detailed derivation is provided in the Appendix A. Usually, we treat the superposition of these infinitely many delta functions as a continuous function, for example, the spectral density of an Ohmic-type heat reservoir with a high cut-off frequency ω_D considered in this paper takes the form [23, 24]

$$J_j(\omega) = \frac{C_j \omega}{1 + (\omega/\omega_D)^2}. \quad (17)$$

This canonical Drude cut-off is an extension of the Ohmic model, where the spectral density is modified to include a frequency-dependent damping factor. This damping factor is often represented as a Lorentzian function, introduces a high-frequency cut-off, effectively limiting the spectral density beyond a certain frequency. This modification is crucial for making the model more realistic by preventing the unphysical divergence of the spectral density at high frequencies. Recalling Eq. (12) and noting that λ_j^2 and $J_j(\omega)$ always appear together as a product in the master equation, we absorb λ_j^2 into $J_j(\omega)$ for simplicity by setting $\gamma_j \equiv C_j \lambda_j^2$ and replacing C_j in Eq. (17) with γ_j .

III. THE STEADY STATES

Based on the master equation (8), one can obtain the steady state by solving $\frac{d\rho}{dt} = 0$. As derived in Appendix B, the steady state of the system in the eigenbasis of H_S has the form of

$$\rho_S = \begin{pmatrix} \rho_{11} & & & \rho_{14} \\ & \rho_{22} & \rho_{23} & \\ & \rho_{32} & \rho_{33} & \\ \rho_{41} & & & \rho_{44} \end{pmatrix}. \quad (18)$$

Instead of numerically calculating ρ_S , we analyzed the steady state using a perturbative approach in Appendix B since the explicit analytical expression is difficult to give directly. We find that $\rho_S^{(0)}$ coincides precisely with the steady state derived from the Lindblad master equation (A14) under the same parameter regime, while $\rho_S^{(2)}$ provides the second-order correction. Regarding positively defined ρ_S , since the steady state $\rho_S^{(0)}$ corresponding to the Lindblad master equation is positive, second-order corrections must preserve the positivity of ρ_S , which is guaranteed by the weak coupling condition $\gamma_j \ll 1$.

To verify the master equation, we first consider two special cases. For $\gamma_2 = 0$ corresponding to the case where

the system is coupled to only one of the two thermal reservoirs, the usual expectation is that the steady state of the system is the Gibbs state, which corresponds to the Lindblad steady state as

$$\rho_S^{(0)} = \tau_S \equiv \frac{\exp(-\beta_1 H_S)}{\text{Tr}(\exp(-\beta_1 H_S))}. \quad (19)$$

However, due to the non-negligible interaction between the system and the environment, the actual steady state corresponds to the MFG state [47–50]

$$\begin{aligned} \rho_S = \tau_S - \beta_1 \sum_\mu \tau_S S(\omega_\mu) \\ \times \left(V_1^\dagger(\omega_\mu) V_1(\omega_\mu) - \text{Tr} \left(\tau_S V_1^\dagger(\omega_\mu) V_1(\omega_\mu) \right) \right) \\ - \sum_{\mu \neq \nu} \frac{1}{\omega_\mu - \omega_\nu} S(\omega_\nu) \\ \times \left(\left[V_1^\dagger(\omega_\mu), V_1(\omega_\nu) \tau_S \right] + \left[\tau_S V_1^\dagger(\omega_\nu), V_1(\omega_\mu) \right] \right) \\ - \sum_\mu \left[V_1(\omega_\mu), \tau_S V_1^\dagger(\omega_\mu) \right] \frac{dS(\omega)}{d\omega} \Big|_{\omega=\omega_\mu}, \end{aligned} \quad (20)$$

where the correction, in this case, precisely matches the second-order correction Eqs. (B4,B5) obtained from the BR master equation. When $\gamma_1 \rightarrow 0$, the correction can be negligible, and the steady state recovers the Gibbs state τ_S . In the second case where $T_1 = T_2 = T$, the system also reaches an equilibrium state corresponding to the other MFG steady state. For both cases, the second-order correction exhibit excellent agreement, as illustrated in Fig. 2.

IV. HEAT CURRENTS

We now focus on the non-equilibrium steady state where $T_2 \neq T_1$ and $\gamma_1 \neq 0, \gamma_2 \neq 0$. In this scenario, the heat spontaneously flows from the high-temperature reservoir to the low-temperature reservoir through the TLAs system. Our primary interest lies in the steady-state heat current $\mathcal{J}_j = \text{Tr}((H_S + H_{LS})\mathcal{L}_j)$.

Based on the BR master equation, one can find that $[H_S, H_{LS}] \neq 0$, but the conservation law remains valid i.e.,

$$\begin{aligned} \mathcal{J}_1 + \mathcal{J}_2 &= \text{Tr}((H_S + H_{LS})(\mathcal{L}_1(\rho_S) + \mathcal{L}_2(\rho_S))) \\ &= i\text{Tr}((H_S + H_{LS})[H_S + H_{LS}, \rho_S]) = 0. \end{aligned} \quad (21)$$

In Fig. 3 and Fig. 4, we plot the heat currents obtained from the BR master equation and the Lindblad master equation, respectively. It is observed that the heat current for the BR master equation is always smaller than that derived from the Lindblad master equation. This reflects the suppressive effect of the non-secular terms on the heat current. In particular, the suppression magnitude increases with the temperature difference when all other parameters remain constant.

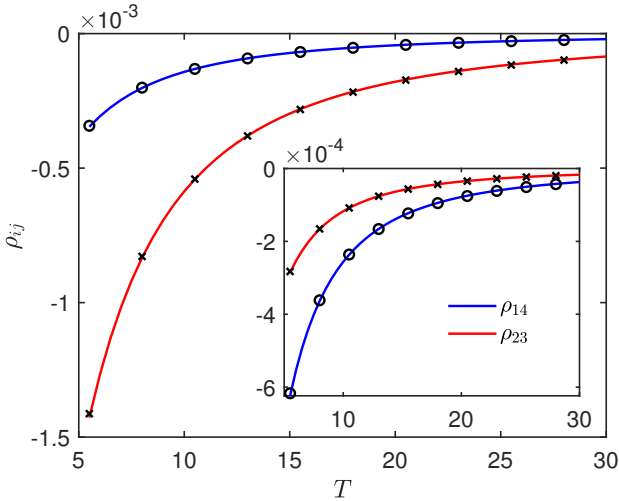


FIG. 2. The secondary diagonal elements of the system's steady state or the mean force Gibbs state ρ_{ij} dependent on the temperature of the thermal reservoirs $T_1 = T_2 = T$. Here we set $\gamma_1 = 0.01$, $\gamma_2 = 0$, $\omega_D = 50$, $\varepsilon_1 = 5$, $\varepsilon_2 = 4$, $g = 1$, only the first thermal reservoir interacts with the system. The blue line represents ρ_{14} ; the red line represents ρ_{23} , and the 'o' and 'x' labeled points represent the corresponding ρ_{ij} of the mean force Gibbs state. For the inset, $\gamma_2 = 0.01$, while keeping all other parameters unchanged, both thermal reservoirs interact with the system for this case.

In addition, Fig. 3 illustrates that the magnitude of suppression in the heat current is negatively correlated with g under fixed parameters. Similarly, Fig. 4 shows that while keeping $\varepsilon_1 + \varepsilon_2$ constant, the magnitude of suppression in the heat current is negatively correlated with $\varepsilon_1 - \varepsilon_2$. Namely, with the eigenenergy β corresponding to the states $|s_1\rangle$ and $|s_4\rangle$ unchanged, the suppression is negatively correlated with the eigenenergy α corresponding to $|s_2\rangle$ and $|s_3\rangle$. This also implies that when $\varepsilon_1 = \varepsilon_2 = \varepsilon$ (i.e., in the symmetric case), the difference between the heat currents predicted by the Lindblad master equation and the BR master equation should be the largest. However, we find that in the symmetric case, the Lindblad master equation loses its validity with a small $g \ll 1$. This is because, under these conditions, the secular approximation—which is a fundamental assumption in deriving the Lindblad master equation—fails to hold: $\omega_1 - \omega_2 = 2\alpha = 2g \sim \tau_R^{-1}$. Although we can still compute the steady-state solution and steady-state heat current for the Lindblad master equation in this scenario, these results lack physical meaning and exhibit unphysical behavior, such as the steady-state heat current not approaching zero as g tends to zero, a more detailed discussion can be found in Appendix C.

Under the symmetric conditions, the BR master equation remains valid and physically meaningful. We plot the heat currents in Fig. 5, which shows that the steady-state heat current significantly decreases as g decreases. It indicates that in the symmetric case, the heat cur-

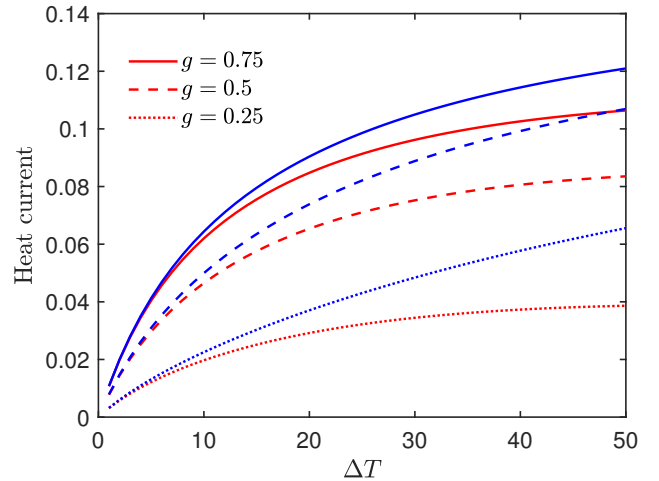


FIG. 3. The heat currents \mathcal{J}_1 vs the temperature difference ΔT . Here we set $T_2 = 5$, $T_1 = 5 + \Delta T$, $\varepsilon_1 = 5$, $\varepsilon_2 = 4$, $\gamma_1 = \gamma_2 = 0.01$, $\omega_D = 50$. The blue lines represent the heat current obtained by the Lindblad master equation, and the red lines represent the heat current obtained by the BR master equation. For the solid, dashed, dotted lines, $g = 0.75$, 0.5 , 0.25 , respectively.

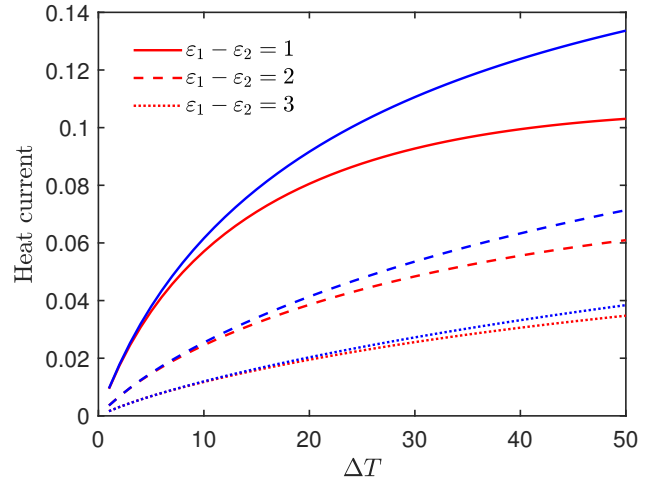


FIG. 4. The heat currents \mathcal{J}_1 vs the temperature difference ΔT . Here we set $T_2 = 5$, $T_1 = 5 + \Delta T$, $\varepsilon_1 + \varepsilon_2 = 10$, $g = 0.5$, $\gamma_1 = \gamma_2 = 0.01$, $\omega_D = 50$. The blue lines represent the heat current obtained by the Lindblad master equation, and the red lines represent the heat current obtained by the BR master equation. For the solid, dashed, dotted lines, $(\varepsilon_1, \varepsilon_2) = (5.5, 4.5)$, $(6, 4)$, $(6.5, 3.5)$, respectively.

rent obtained from the BR master equation vanishes as g tends to zero (see Appendix C for a detailed derivation). Furthermore, one can find that the increase in ε amplifies the heat current. As the temperature difference increases, the heat current initially rises and then decreases, exhibiting the NDTC effect. In fact, the NDTC exists in the asymmetric case as well. It only requires a

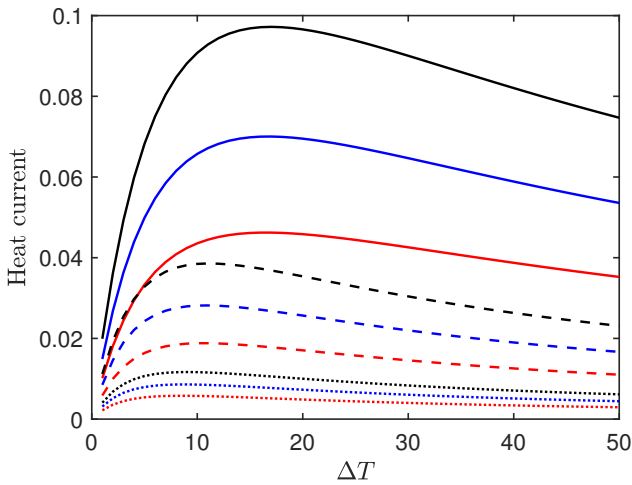


FIG. 5. The heat currents \mathcal{J}_1 versus the temperature difference ΔT . Here we set $T_2 = 5, T_1 = 5 + \Delta T, \gamma_1 = \gamma_2 = 0.01, \omega_D = 50$. For the red, blue, and black lines, the parameters are $(\varepsilon_1, \varepsilon_2) = (4, 4), (5, 5)$, and $(6, 6)$ respectively, while for the solid, dashed, and dotted lines, $g = 0.2, 0.1$, and 0.05 respectively.

larger temperature difference or a larger γ compared to the symmetric case as shown in Fig. 6. As γ increases, the NDTC effect becomes more pronounced, which is caused by BR's correction to the Lindblad master equation.

Considering the heat current based on the BR master equation, we can expand the density matrix to the second order as $\rho^{BR} = \rho^L + \lambda^2 \rho^{(2)} + \dots$. Thus the heat current can be given as

$$\begin{aligned} \mathcal{J}_j^{BR} &= \text{Tr}((H_S + H_{LS}^{BR}) \mathcal{L}_j^{BR}(\rho^{BR})) \\ &= \mathcal{J}_j^L + \lambda^2 \text{Tr} \left((H_S + H_{LS}^{BR}) \mathcal{L}_j^{BR} \left(\rho^{(2)} + \dots \right) \right) \quad (22) \end{aligned}$$

where

$$\begin{aligned} \mathcal{J}_j^L &= \text{Tr} \left((H_S + H_{LS}^{BR}) \mathcal{L}_j^{BR}(\rho^L) \right) \\ &= \text{Tr} \left((H_S + H_{LS}^L) \mathcal{L}_j^L(\rho^L) \right). \quad (23) \end{aligned}$$

Eq. (22) shows that the corrections to the heat current arise entirely from the second and higher-order contributions of the steady-state solution. Consequently, if only the zeroth-order approximation is considered, the magnitude of the heat current predicted by the BR master equation does not differ from that given by the Lindblad master equation despite the explicit inclusion of non-secular terms in the former.

In our model, it can be shown that the NDTC emerges exclusively in the BR master equation, which can be verified as follows. The heat current derived from the Lindblad master equation is given by

$$\mathcal{J}_1^L = \sum_{i=1}^2 A_i (\bar{n}_1(\omega_i) - \bar{n}_2(\omega_i)) (\omega_i + \delta_i), \quad (24)$$

with

$$A_1 = 2 \sin^2 \phi_+ \cos^2 \phi_- \frac{J_1(\omega_1) J_2(\omega_1)}{\tilde{G}_+(\omega_1) + \tilde{G}_+(-\omega_1)}, \quad (25)$$

$$A_2 = 2 \sin^2 \phi_- \cos^2 \phi_+ \frac{J_1(\omega_2) J_2(\omega_2)}{\tilde{G}_+(\omega_2) + \tilde{G}_+(-\omega_2)}, \quad (26)$$

and δ_i are second-order corrections to the eigenfrequency ω_i introduced by the lamb shift. We can prove that when T_2 is fixed and $T_1 > T_2, \partial \mathcal{J}_1^L / \partial T_1 > 0$, which shows that the heat current given by Lindblad's master equation does not exhibit the NDTC effect.

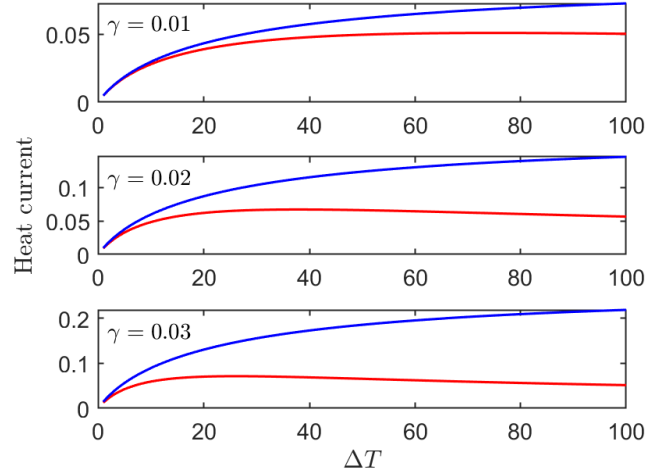


FIG. 6. The heat currents \mathcal{J}_1 vs the temperature difference ΔT . Here we set $T_2 = 5, T_1 = 5 + \Delta T, \varepsilon_1 = 4, \varepsilon_2 = 3, g = 0.5, \omega_D = 50$. For the first inset, $\gamma_1 = \gamma_2 = 0.01$; for the second inset, $\gamma_1 = \gamma_2 = 0.02$; for the third inset, $\gamma_1 = \gamma_2 = 0.03$. The blue and red lines represent the heat currents obtained using the Lindblad and BR master equations, respectively.

V. CONCLUSIONS

We have studied the heat currents through a coupled TLA system based on the BR master equation under the Born-Markov approximation. Using a perturbative approach, we yield analytical expressions of the steady-state density matrix at zeroth and second order. The zeroth-order solution coincides precisely with the steady-state density matrix of the Lindblad master equation, and the second-order solution aligns with the mean force Gibbs state when an equilibrium state exists in the regime. By studying the heat current in our regime, we discovered that the non-secular terms exert a suppressive effect on the heat current, and the magnitude of this suppression is negatively correlated with g and $\varepsilon_1 - \varepsilon_2$. In particular, we identified the emergence of NDTC, which is a key nonlinear transport feature, in specific parameter regimes within the BR formalism. This phenomenon,

absent in the Lindblad description, manifests as a decrease in heat current with increasing temperature bias, highlighting the essential role of coherence and quantum correlations in shaping thermal response. Furthermore, it shows that in the symmetric case, the Lindblad master equation yields unphysical results as g approaches zero, whereas the BR master equation remains valid regardless of the coupling strength.

In summary, this work demonstrates the critical importance of non-secular contributions in capturing realistic quantum thermal transport phenomena, particularly the emergence of NDTC. Additionally, we also find that the concurrence of assistance and the linear entropy have behaviors similar to those of the NDTC, which is not pro-

vided here. Our findings highlight the benefits of the Bloch-Redfield formalism in describing the dynamics of open quantum systems beyond the secular approximation, thereby paving the way for more accurate modeling and control of heat flow in quantum thermal devices.

ACKNOWLEDGMENTS

This work was supported by the National Natural Science Foundation of China under Grants Nos. 12175029.

REFERENCES

- [1] T. Feldmann and R. Kosloff, Performance of discrete heat engines and heat pumps in finite time, *Phys. Rev. E* **61**, 4774 (2000).
- [2] D. Segal and A. Nitzan, Molecular heat pump, *Phys. Rev. E* **73**, 026109 (2006).
- [3] E. Geva and R. Kosloff, A quantum-mechanical heat engine operating in finite time. a model consisting of spin-1/2 systems as the working fluid, *The Journal of Chemical Physics* **96**, 3054 (1992), <https://doi.org/10.1063/1.461951>.
- [4] K. Ono, S. N. Shevchenko, T. Mori, S. Moriyama, and F. Nori, Analog of a quantum heat engine using a single-spin qubit, *Phys. Rev. Lett.* **125**, 166802 (2020).
- [5] M. Naghiloo, D. Tan, P. M. Harrington, J. J. Alonso, E. Lutz, A. Romito, and K. W. Murch, Heat and work along individual trajectories of a quantum bit, *Phys. Rev. Lett.* **124**, 110604 (2020).
- [6] M. Josefsson and M. Leijnse, Double quantum-dot engine fueled by entanglement between electron spins, *Phys. Rev. B* **101**, 081408 (2020).
- [7] R. Dann, R. Kosloff, and P. Salamon, Quantum finite-time thermodynamics: Insight from a single qubit engine, *Entropy* **22**, 10.3390/e22111255 (2020).
- [8] O. Maillet, P. A. Erdman, V. Cavina, B. Bhandari, E. T. Mannila, J. T. Peltonen, A. Mari, F. Taddei, C. Jarzynski, V. Giovannetti, and J. P. Pekola, Optimal probabilistic work extraction beyond the free energy difference with a single-electron device, *Phys. Rev. Lett.* **122**, 150604 (2019).
- [9] L. d. S. Souza, G. Manzano, R. Fazio, and F. Iemini, Collective effects on the performance and stability of quantum heat engines, *Phys. Rev. E* **106**, 014143 (2022).
- [10] A. Colla and H.-P. Breuer, Thermodynamic roles of quantum environments: from heat baths to work reservoirs, *Quantum Science and Technology* **10**, 015047 (2024).
- [11] J. P. Palao, R. Kosloff, and J. M. Gordon, Quantum thermodynamic cooling cycle, *Phys. Rev. E* **64**, 056130 (2001).
- [12] T. Feldmann, E. Geva, R. Kosloff, and P. Salamon, Heat engines in finite time governed by master equations, *American Journal of Physics* **64**, 485 (1996), <https://doi.org/10.1119/1.18197>.
- [13] P. Skrzypczyk, N. Brunner, N. Linden, and S. Popescu, The smallest refrigerators can reach maximal efficiency, *Journal of Physics A: Mathematical and Theoretical* **44**, 492002 (2011).
- [14] C.-s. Yu and Q.-y. Zhu, Re-examining the self-contained quantum refrigerator in the strong-coupling regime, *Physical Review E* **90**, 052142 (2014).
- [15] C. Yu, B. Guo, and T. Liu, Quantum self-contained refrigerator in terms of the cavity quantum electrodynamics in the weak internal-coupling regime., *Optics Express* **27**, 6863 (2019).
- [16] L. Buffoni, A. Solfanelli, P. Verrucchi, A. Cuccoli, and M. Campisi, Quantum measurement cooling, *Phys. Rev. Lett.* **122**, 070603 (2019).
- [17] R. R. Soldati, D. B. R. Dasari, J. Wrachtrup, and E. Lutz, Thermodynamics of a minimal algorithmic cooling refrigerator, *Phys. Rev. Lett.* **129**, 030601 (2022).
- [18] B. Bhandari and A. N. Jordan, Continuous measurement boosted adiabatic quantum thermal machines, *Phys. Rev. Res.* **4**, 033103 (2022).
- [19] C. Elouard, D. Herrera-Martí, B. Huard, and A. Auffèves, Extracting work from quantum measurement in maxwell's demon engines, *Phys. Rev. Lett.* **118**, 260603 (2017).
- [20] K. Yanik, B. Bhandari, S. K. Manikandan, and A. N. Jordan, Thermodynamics of quantum measurement and maxwell's demon's arrow of time, *Phys. Rev. A* **106**, 042221 (2022).
- [21] K. Jacobs, Second law of thermodynamics and quantum feedback control: Maxwell's demon with weak measurements, *Phys. Rev. A* **80**, 012322 (2009).
- [22] F.-J. Chan, Y.-T. Huang, J.-D. Lin, H.-Y. Ku, J.-S. Chen, H.-B. Chen, and Y.-N. Chen, Maxwell's two-demon engine under pure dephasing noise, *Phys. Rev. A* **106**, 052201 (2022).
- [23] H.-P. Breuer, F. Petruccione, *et al.*, *The theory of open quantum systems* (Oxford University Press on Demand, 2002).
- [24] U. Weiss, *Quantum dissipative systems* (World Scientific, 2012).
- [25] H. J. Carmichael, *Statistical methods in quantum optics 1: master equations and Fokker-Planck equations* (Springer Science & Business Media, 2013).

[26] G. Schaller, Non-equilibrium master equations, Lecture Notes TU Berlin, Berlin (2014).

[27] D. A. Lidar, Lecture notes on the theory of open quantum systems, arXiv preprint arXiv:1902.00967 (2019).

[28] I. Oppenheim and K. E. Shuler, Master equations and markov processes, *Phys. Rev.* **138**, B1007 (1965).

[29] A. Rivas, A. D. K. Plato, S. F. Huelga, and M. B. Plenio, Markovian master equations: a critical study, *New Journal of Physics* **12**, 113032 (2010).

[30] T. Albash, S. Boixo, D. A. Lidar, and P. Zanardi, Quantum adiabatic markovian master equations, *New Journal of Physics* **14**, 123016 (2012).

[31] C. Gardiner and P. Zoller, *Quantum noise: a handbook of Markovian and non-Markovian quantum stochastic methods with applications to quantum optics* (Springer Science & Business Media, 2004).

[32] E. Mozgunov and D. Lidar, Completely positive master equation for arbitrary driving and small level spacing, *Quantum* **4**, 227 (2020).

[33] R. Harris, Encyclopedia of nuclear magnetic resonance, in-Chief DM Grant and RK Harris **5**, 3301 (1996).

[34] A. Ishizaki and G. R. Fleming, On the adequacy of the redfield equation and related approaches to the study of quantum dynamics in electronic energy transfer, *The Journal of chemical physics* **130** (2009).

[35] W. T. Pollard, A. K. Felts, and R. A. Friesner, The redfield equation in condensed-phase quantum dynamics, *Advances in Chemical Physics* (John Wiley & Sons, Inc., 2007) pp , 77 (1996).

[36] J. Gemmer, M. Michel, and G. Mahler, *Quantum thermodynamics: Emergence of thermodynamic behavior within composite quantum systems*, Vol. 784 (Springer, 2009).

[37] R. Alicki, D. A. Lidar, and P. Zanardi, Internal consistency of fault-tolerant quantum error correction in light of rigorous derivations of the quantum markovian limit, *Physical Review A* **73**, 052311 (2006).

[38] K. Ptaszyński and M. Esposito, Thermodynamics of quantum information flows, *Phys. Rev. Lett.* **122**, 150603 (2019).

[39] S.-Y. Wang, Q. Yang, and F.-L. Zhang, Thermodynamically consistent master equation based on subsystem eigenstates, *Phys. Rev. E* **107**, 014108 (2023).

[40] A. REDFIELD, The theory of relaxation processes, in *Advances in Magnetic Resonance*, Advances in Magnetic and Optical Resonance, Vol. 1, edited by J. S. Waugh (Academic Press, 1965) pp. 1–32.

[41] A. G. Redfield, On the theory of relaxation processes, *IBM Journal of Research and Development* **1**, 19 (1957).

[42] G. Lindblad, On the generators of quantum dynamical semigroups, *Communications in mathematical physics* **48**, 119 (1976).

[43] E. B. Davies, Markovian master equations, *Communications in mathematical Physics* **39**, 91 (1974).

[44] V. Gorini, A. Kossakowski, and E. C. G. Sudarshan, Completely positive dynamical semigroups of n-level systems, *Journal of Mathematical Physics* **17**, 821 (1976).

[45] V. Vadimov, J. Tuorila, T. Orell, J. Stockburger, T. Alani-Nissila, J. Ankerhold, and M. Möttönen, Validity of born-markov master equations for single- and two-qubit systems, *Phys. Rev. B* **103**, 214308 (2021).

[46] D. Davidović, Completely positive, simple, and possibly highly accurate approximation of the redfield equation, *Quantum* **4**, 326 (2020).

[47] J. S. Lee and J. Yeo, Perturbative steady states of completely positive quantum master equations, *Phys. Rev. E* **106**, 054145 (2022).

[48] A. S. Trushechkin, M. Merkli, J. D. Cresser, and J. Anders, Open quantum system dynamics and the mean force gibbs state, *AVS Quantum Science* **4**, 012301 (2022), https://pubs.aip.org/avs/aqs/article-pdf/doi/10.1116/5.0073853/19803511/012301_1_online.pdf.

[49] J. D. Cresser and J. Anders, Weak and ultrastrong coupling limits of the quantum mean force gibbs state, *Phys. Rev. Lett.* **127**, 250601 (2021).

[50] J. Thingna, J.-S. Wang, and P. Hänggi, Generalized gibbs state with modified redfield solution: Exact agreement up to second order, *The Journal of Chemical Physics* **136**, 194110 (2012), https://pubs.aip.org/aip/jcp/article-pdf/doi/10.1063/1.4718706/15449334/194110_1_online.pdf.

[51] D. Segal, Heat flow in nonlinear molecular junctions: Master equation analysis, *Phys. Rev. B* **73**, 205415 (2006).

[52] X. Cao, C. Wang, H. Zheng, and D. He, Quantum thermal transport via a canonically transformed redfield approach, *Phys. Rev. B* **103**, 075407 (2021).

[53] S. S. Dey, G. Timossi, L. Amico, and G. Marchegiani, Negative differential thermal conductance by photonic transport in electronic circuits, *Phys. Rev. B* **107**, 134510 (2023).

[54] H. Liu, C. Wang, L.-Q. Wang, and J. Ren, Strong system-bath coupling induces negative differential thermal conductance and heat amplification in nonequilibrium two-qubit systems, *Phys. Rev. E* **99**, 032114 (2019).

[55] K. Joulain, Y. Ezzahri, J. Drevillon, and P. Ben-Abdallah, Modulation and amplification of radiative far field heat transfer: Towards a simple radiative thermal transistor, *Applied Physics Letters* **106**, 133505 (2015).

[56] N. Li, J. Ren, L. Wang, G. Zhang, P. Hänggi, and B. Li, Colloquium: Phononics: Manipulating heat flow with electronic analogs and beyond, *Rev. Mod. Phys.* **84**, 1045 (2012).

[57] J. Ordóñez-Miranda, Y. Ezzahri, and K. Joulain, Quantum thermal diode based on two interacting spinlike systems under different excitations, *Phys. Rev. E* **95**, 022128 (2017).

[58] C. Karg 1, M. T. Naseem, T. c. v. Opatrný, O. E. Müstecaplıoğlu, and G. Kurizki, Quantum optical two-atom thermal diode, *Phys. Rev. E* **99**, 042121 (2019).

[59] C. Wang, D. Xu, H. Liu, and X. Gao, Thermal rectification and heat amplification in a nonequilibrium v-type three-level system, *Phys. Rev. E* **99**, 042102 (2019).

[60] L. Tesser, B. Bhandari, P. A. Erdman, E. Paladino, R. Fazio, and F. Taddei, Heat rectification through single and coupled quantum dots, *New Journal of Physics* **24**, 035001 (2022).

[61] V. Balachandran, G. Benenti, E. Pereira, G. Casati, and D. Poletti, Perfect diode in quantum spin chains, *Phys. Rev. Lett.* **120**, 200603 (2018).

[62] D. Segal, Single mode heat rectifier: Controlling energy flow between electronic conductors, *Phys. Rev. Lett.* **100**, 105901 (2008).

[63] M. Terraneo, M. Peyrard, and G. Casati, Controlling the energy flow in nonlinear lattices: A model for a thermal rectifier, *Phys. Rev. Lett.* **88**, 094302 (2002).

[64] E. Pereira, Sufficient conditions for thermal rectification in general graded materials, *Phys. Rev. E* **83**, 031106 (2011).

[65] J. Yang, C. Elouard, J. Splettstoesser, B. Sothmann, R. Sánchez, and A. N. Jordan, Thermal transistor and thermometer based on coulomb-coupled conductors, *Phys. Rev. B* **100**, 045418 (2019).

[66] K. V. Hovhannisyan and A. Imparato, Quantum current in dissipative systems, *New Journal of Physics* **21**, 052001 (2019).

[67] L. Quiroga, F. J. Rodriguez, M. E. Ramírez, and R. París, Nonequilibrium thermal entanglement, *Phys. Rev. A* **75**, 032308 (2007).

[68] I. Sinaysky, F. Petruccione, and D. Burgarth, Dynamics of nonequilibrium thermal entanglement, *Phys. Rev. A* **78**, 062301 (2008).

[69] Y.-j. Yang, Y.-q. Liu, and C.-s. Yu, Heat transfer in transversely coupled qubits: optically controlled thermal modulator with common reservoirs, *Journal of Physics A: Mathematical and Theoretical* **55**, 395303 (2022).

[70] L.-Z. Hu, Z.-X. Man, and Y.-J. Xia, Steady-state entanglement and thermalization of coupled qubits in two common heat baths, *Quantum Information Processing* **17**, 1 (2018).

[71] M. Cattaneo, G. L. Giorgi, S. Maniscalco, and R. Zambrini, Local versus global master equation with common and separate baths: superiority of the global approach in partial secular approximation, *New Journal of Physics* **21**, 113045 (2019).

[72] Z. Wang, W. Wu, and J. Wang, Steady-state entanglement and coherence of two coupled qubits in equilibrium and nonequilibrium environments, *Phys. Rev. A* **99**, 042320 (2019).

[73] T. Novotný, Investigation of apparent violation of the second law of thermodynamics in quantum transport studies, *Europhysics Letters* **59**, 648 (2002).

[74] A. Levy and R. Kosloff, The local approach to quantum transport may violate the second law of thermodynamics, *Europhysics Letters* **107**, 20004 (2014).

Appendix A: The Derivation of the master equation

In the interaction picture, the von Neumann equation describes the evolution of the entire regime, encompassing both the system and its environment.

$$\frac{d\rho'(t)}{dt} = -i [H_I(t), \rho'(t)]. \quad (\text{A1})$$

where $\rho'(t)$ denotes the total density matrix, and we can decompose the interaction Hamiltonian $H_I = \lambda \sum_{j,\mu} V_j(\omega_\mu) \otimes B_j^x$. With the standard procedure of Born-Markov approximation, we can get the evolution of the reduced density matrix $\rho(t)$ as

$$\frac{d\rho(t)}{dt} = \sum_{\mu,i,j} \Gamma_{i,j}(\omega_\mu) [V_j(\omega_\mu) \rho(t), V_i^\dagger(\omega_\mu)] + \sum_{\mu,i,j} \Gamma_{j,i}^*(\omega_\mu) [V_j(\omega_\mu), \rho(t) V_i^\dagger(\omega_\mu)], \quad (\text{A2})$$

where

$$\Gamma_{i,j}(\omega_\mu) = \int_0^\infty ds e^{i\omega_\mu s} \langle B_i^x(s) B_j^x \rangle \quad (\text{A3})$$

is the forward Fourier transform of the reservoir correlation function $\langle B_i^x(s) B_j^x \rangle$. Actually only the terms $\langle B_j^x(s) B_j^x \rangle$ are not zero, which can be expressed as

$$\begin{aligned} \text{Tr} (B_j^x(s) B_j^x \rho_B) &= \sum_n |\kappa_{j,n}|^2 (e^{-i\omega_n s} (\bar{n}_j(\omega_n) + 1) + e^{i\omega_n s} \bar{n}_j(\omega_n)) \\ &= \frac{1}{\pi} \int_0^\infty J_j(\omega) (e^{-i\omega s} (\bar{n}_j(\omega) + 1) + e^{i\omega s} \bar{n}_j(\omega)) d\omega, \end{aligned} \quad (\text{A4})$$

so we can obtain that

$$\begin{aligned}
\Gamma_{j,j}(\omega_\mu) \equiv \Gamma_j(\omega_\mu) &= \int_0^\infty ds e^{i\omega_\mu s} \text{Tr} (B_j^x(s) B_j^x \rho_B) \\
&= \frac{1}{\pi} \int_0^\infty \left(\int_0^\infty e^{-i(\omega-\omega_\mu)s} ds \right) J_j(\omega) (\bar{n}_j(\omega) + 1) d\omega \\
&\quad + \frac{1}{\pi} \int_0^\infty \left(\int_0^\infty e^{-i(-\omega_\mu-\omega)s} ds \right) J_j(\omega) \bar{n}_j(\omega) d\omega.
\end{aligned} \tag{A5}$$

Using the Kramers-Kronig relations

$$\int_0^\infty e^{-i(\omega-\omega_0)s} ds = \pi\delta(\omega - \omega_0) - iP.V. \frac{1}{\omega - \omega_0}, \tag{A6}$$

and by the properties of the delta function

$$\int_0^\infty \delta(\omega - \omega_\mu) J_j(\omega) (\bar{n}_j(\omega) + 1) d\omega = J_j(\omega_\mu) (\bar{n}_j(\omega_\mu) + 1), \tag{A7}$$

$$\int_0^\infty \delta(\omega + \omega_\mu) J_j(\omega) \bar{n}_j(\omega) d\omega = 0, \tag{A8}$$

we can obtain

$$\Gamma_j(\omega_\mu) = J_j(\omega_\mu) (\bar{n}_j(\omega_\mu) + 1) + \frac{i}{\pi} P.V. \int_0^\infty J_j(\omega) \left(\frac{\bar{n}_j(\omega) + 1}{\omega_\mu - \omega} + \frac{\bar{n}_j(\omega)}{\omega_\mu + \omega} \right) d\omega, \tag{A9}$$

$$\Gamma_j(-\omega_\mu) = J_j(\omega_\mu) \bar{n}(\omega_\mu) - \frac{i}{\pi} P.V. \int_0^\infty J_j(\omega) \left(\frac{\bar{n}_j(\omega)}{\omega_\mu - \omega} + \frac{\bar{n}_j(\omega) + 1}{\omega_\mu + \omega} \right) d\omega, \tag{A10}$$

where the *P.V.* denotes the Cauchy principal value.

Reorganising the terms in Eq. (A2) in Schrödinger picture, we eventually arrive at

$$\frac{d\rho}{dt} = -i [H_S + H_{LS}, \rho] + \sum_j \mathcal{L}_j(\rho), \tag{A11}$$

where

$$H_{LS} = \sum_j \sum_{\omega, \omega'} \xi_j(\omega, \omega') V_j^\dagger(\omega') V_j(\omega), \tag{A12}$$

$$\mathcal{L}_j(\rho) = \sum_{\omega, \omega'} \gamma_j(\omega, \omega') \left(V_j(\omega) \rho V_j^\dagger(\omega') - \frac{1}{2} \{ V_j^\dagger(\omega') V_j(\omega), \rho \} \right). \tag{A13}$$

If $|\omega - \omega'| \gg \tau_R^{-1} \sim \lambda^2$, we can apply the secular approximation here, ignoring the terms where ω and ω' are different, we get the Lindblad master equation as

$$H_{LS}^L = \sum_{j, \omega} \xi_j(\omega, \omega) V_j^\dagger(\omega) V_j(\omega), \tag{A14}$$

$$\mathcal{L}_j^L(\rho) = \sum_{\omega} \gamma_j(\omega, \omega) \left(V_j(\omega) \rho V_j^\dagger(\omega) - \frac{1}{2} \{ V_j^\dagger(\omega) V_j(\omega), \rho \} \right). \quad (\text{A15})$$

According to Eqs. (A9, A10), we have

$$\gamma_j(\omega, \omega) = 2G_j(\omega) = 2J_j(\omega)(\bar{n}_j(\omega) + 1), \quad (\text{A16})$$

$$\xi_j(\omega, \omega) = S_j(\omega) = \frac{1}{\pi} P.V. \int_0^\infty J_j(\omega') \left(\frac{\bar{n}_j(\omega') + 1}{\omega - \omega'} + \frac{\bar{n}_j(\omega')}{\omega + \omega'} \right) d\omega', \quad (\text{A17})$$

where the KMS condition is satisfied, i.e.,

$$\gamma_j(-\omega, -\omega) = 2G_j(-\omega) = 2e^{-\beta_j \omega} G_j(\omega) = e^{-\beta_j \omega} \gamma_j(\omega, \omega). \quad (\text{A18})$$

Appendix B: The steady states of the Bloch-Redfield master equation

By substituting the eigenoperators into the master equation Eq. (A11) and making simplification, we find that the evolution of the density matrix of the system decouples into two parts:

$$\rho_S = \begin{pmatrix} \rho_{11} & & \rho_{14} & \\ & \rho_{22} & \rho_{23} & \\ & \rho_{32} & \rho_{33} & \\ \rho_{41} & & & \rho_{44} \end{pmatrix}, \quad \rho_O = \begin{pmatrix} & \rho_{12} & \rho_{13} & \\ \rho_{21} & & & \rho_{24} \\ \rho_{31} & & & \rho_{34} \\ & \rho_{42} & \rho_{43} & \end{pmatrix},$$

ρ_S consists of the elements on the primary and secondary diagonals of the density matrix, and ρ_O consists of the remaining elements. They both evolved independently as

$$\frac{d}{dt} \rho_S = M_{11}\rho_{11} + M_{22}\rho_{22} + M_{33}\rho_{33} + M_{44}\rho_{44} + M_{14}\rho_{14} + M_{23}\rho_{23} + M_{32}\rho_{32} + M_{41}\rho_{41}, \quad (\text{B1})$$

$$\frac{d}{dt} \rho_O = M_{12}\rho_{12} + M_{13}\rho_{13} + M_{21}\rho_{21} + M_{24}\rho_{24} + M_{31}\rho_{31} + M_{34}\rho_{34} + M_{42}\rho_{42} + M_{43}\rho_{43}, \quad (\text{B2})$$

where the explicit expressions for M_{ij} are given as follows. First we introduce some notation to simplify the result. For $F \in \{G, S\}$,

$$\begin{aligned} \bar{F}_1(\omega) &\equiv F_1(\omega) \sin \phi_+ \cos \phi_+, \forall \omega; \bar{F}_2(\omega) \equiv F_2(\omega) \sin \phi_- \cos \phi_-, \forall \omega; \\ \tilde{F}_1(\omega) &\equiv F_1(\omega) \sin^2 \phi_+, \omega = \pm \omega_1; \tilde{F}_1(\omega) \equiv F_1(\omega) \cos^2 \phi_+, \omega = \pm \omega_2; \\ \tilde{F}_2(\omega) &\equiv F_2(\omega) \cos^2 \phi_-, \omega = \pm \omega_1; \tilde{F}_2(\omega) \equiv F_2(\omega) \sin^2 \phi_-, \omega = \pm \omega_2; \\ \bar{F}_\pm &= \bar{F}_1 \pm \bar{F}_2, \tilde{F}_\pm = \tilde{F}_1 \pm \tilde{F}_2. \end{aligned}$$

Then the expressions for M_{ij} are

$$M_{11} = \begin{pmatrix} -2\tilde{G}_+(\omega_1) - 2\tilde{G}_+(\omega_2) & 0 & 0 & M_{11}(1, 4) \\ 0 & 2\tilde{G}_+(\omega_1) & M_{11}(2, 3) & 0 \\ 0 & M_{11}^*(2, 3) & 2\tilde{G}_+(\omega_2) & 0 \\ M_{11}^*(1, 4) & 0 & 0 & 0 \end{pmatrix},$$

$$M_{11}(1, 4) = \bar{G}_+(\omega_2) - \bar{G}_+(\omega_1) + i\bar{S}_+(\omega_1) - i\bar{S}_+(\omega_2),$$

$$M_{11}(2, 3) = \bar{G}_-(\omega_1) + \bar{G}_-(\omega_2) + i\bar{S}_-(\omega_1) - i\bar{S}_-(\omega_2);$$

$$M_{22} = \begin{pmatrix} 2\tilde{G}_+(-\omega_1) & 0 & 0 & M_{22}(1, 4) \\ 0 & -2\tilde{G}_+(-\omega_1) - 2\tilde{G}_+(\omega_2) & M_{22}(2, 3) & 0 \\ 0 & M_{22}^*(2, 3) & 0 & 0 \\ M_{22}^*(1, 4) & 0 & 0 & 2\tilde{G}_+(\omega_2) \end{pmatrix},$$

$$M_{22}(1, 4) = \bar{G}_+(-\omega_1) + \bar{G}_+(\omega_2) + i\bar{S}_+(-\omega_1) - i\bar{S}_+(\omega_2),$$

$$M_{22}(2, 3) = \bar{G}_-(\omega_2) - \bar{G}_-(-\omega_1) + i\bar{S}_-(-\omega_1) - i\bar{S}_-(\omega_2);$$

$$M_{33} = \begin{pmatrix} 2\tilde{G}_+(-\omega_2) & 0 & 0 & M_{33}(1,4) \\ 0 & 0 & M_{33}(2,3) & 0 \\ 0 & M_{33}^*(2,3) & -2\tilde{G}_+(\omega_1) - 2\tilde{G}_+(-\omega_2) & 0 \\ M_{33}^*(1,4) & 0 & 0 & 2\tilde{G}_+(\omega_1) \end{pmatrix},$$

$$M_{33}(1,4) = -\bar{G}_+(\omega_1) - \bar{G}_+(-\omega_2) + i\bar{S}_+(\omega_1) - i\bar{S}_+(-\omega_2),$$

$$M_{33}(2,3) = \bar{G}_-(\omega_1) - \bar{G}_-(-\omega_2) + i\bar{S}_-(\omega_1) - i\bar{S}_-(-\omega_2);$$

$$M_{44} = \begin{pmatrix} 0 & 0 & 0 & M_{44}(1,4) \\ 0 & 2\tilde{G}_+(-\omega_2) & M_{44}(2,3) & 0 \\ 0 & M_{44}^*(2,3) & 2\tilde{G}_+(-\omega_1) & 0 \\ M_{44}^*(1,4) & 0 & 0 & -2\tilde{G}_+(-\omega_1) - 2\tilde{G}_+(-\omega_2) \end{pmatrix},$$

$$M_{44}(1,4) = \bar{G}_+(\omega_1) - \bar{G}_+(-\omega_2) + i\bar{S}_+(\omega_1) - i\bar{S}_+(-\omega_2),$$

$$M_{44}(2,3) = -\bar{G}_-(-\omega_1) - \bar{G}_-(-\omega_2) + i\bar{S}_-(-\omega_1) - i\bar{S}_-(-\omega_2);$$

$$M_{14} = \begin{pmatrix} M_{44}^*(1,4) & 0 & 0 & M_{14}(1,4) \\ 0 & -M_{33}^*(1,4) & M_{14}(2,3) & 0 \\ 0 & M_{14}(3,2) & -M_{22}^*(1,4) & 0 \\ 0 & 0 & 0 & M_{11}^*(1,4) \end{pmatrix},$$

$$M_{14}(1,4) = -\left(\tilde{G}_+(\omega_1) + \tilde{G}_+(\omega_2) + \tilde{G}_+(-\omega_1) + \tilde{G}_+(-\omega_2)\right)$$

$$+i\tilde{S}_+(-\omega_1) + i\tilde{S}_+(-\omega_2) - i\tilde{S}_+(\omega_1) - i\tilde{S}_+(\omega_2) - 2i\beta,$$

$$M_{14}(2,3) = -\left(\tilde{G}_-(\omega_1) + \tilde{G}_-(-\omega_1)\right) + i\tilde{S}_-(-\omega_1) - i\tilde{S}_-(\omega_1),$$

$$M_{14}(3,2) = \tilde{G}_-(\omega_2) + \tilde{G}_-(-\omega_2) + i\tilde{S}_-(\omega_2) - i\tilde{S}_-(-\omega_2);$$

$$M_{23} = \begin{pmatrix} -M_{44}^*(2,3) & 0 & 0 & M_{14}^*(2,3) \\ 0 & M_{33}^*(2,3) & M_{23}(2,3) & 0 \\ 0 & 0 & M_{22}^*(2,3) & 0 \\ M_{14}(3,2) & 0 & 0 & -M_{11}^*(2,3) \end{pmatrix},$$

$$M_{23}(2,3) = -\left(\tilde{G}_+(\omega_1) + \tilde{G}_+(\omega_2) + \tilde{G}_+(-\omega_1) + \tilde{G}_+(-\omega_2)\right)$$

$$-i\tilde{S}_+(-\omega_1) + i\tilde{S}_+(-\omega_2) + i\tilde{S}_+(\omega_1) - i\tilde{S}_+(\omega_2) - 2i\alpha;$$

$$M_{41} = M_{14}^\dagger, M_{32} = M_{23}^\dagger;$$

$$M_{12} = \begin{pmatrix} 0 & M_{12}(1,2) & M_{22}(2,3) & 0 \\ M_{12}(2,1) & 0 & 0 & M_{12}(2,4) \\ M_{12}(3,1) & 0 & 0 & 2\tilde{G}_-(\omega_2) \\ 0 & M_{11}^*(1,4) & 0 & 0 \end{pmatrix},$$

$$M_{12}(1,2) = -\left(\tilde{G}_+(-\omega_1) + \tilde{G}_+(\omega_1) + 2\tilde{G}_+(\omega_2)\right) + i\left(\alpha - \beta + \tilde{S}_+(-\omega_1) - \tilde{S}_+(\omega_1)\right),$$

$$M_{12}(2,1) = \tilde{G}_+(\omega_1) + \tilde{G}_+(-\omega_1) + i\tilde{S}_+(\omega_1) - i\tilde{S}_+(-\omega_1),$$

$$M_{12}(2,4) = \bar{G}_+(\omega_1) + \bar{G}_+(\omega_2) + i\bar{S}_+(\omega_1) - i\bar{S}_+(\omega_2),$$

$$M_{12}(3,1) = \bar{G}_-(-\omega_1) + \bar{G}_-(-\omega_2) + i\bar{S}_-(-\omega_1) - i\bar{S}_-(-\omega_2);$$

$$M_{13} = \begin{pmatrix} 0 & M_{33}^*(2,3) & M_{13}(1,3) & 0 \\ M_{13}(2,1) & 0 & 0 & -2\tilde{G}_-(\omega_1) \\ M_{13}(3,1) & 0 & 0 & M_{13}(3,4) \\ 0 & 0 & M_{11}^*(1,4) & 0 \end{pmatrix},$$

$$M_{13}(1,3) = -\left(\tilde{G}_+(\omega_2) + \tilde{G}_+(-\omega_2) + 2\tilde{G}_+(\omega_1)\right) - i\left(\alpha + \beta + \tilde{S}_+(\omega_2) - \tilde{S}_+(-\omega_2)\right),$$

$$M_{13}(2,1) = \bar{G}_-(\omega_1) + \bar{G}_-(-\omega_2) + i\bar{S}_-(\omega_1) - i\bar{S}_-(-\omega_2),$$

$$M_{13}(3,1) = \tilde{G}_+(\omega_2) + \tilde{G}_+(-\omega_2) + i\tilde{S}_+(\omega_2) - i\tilde{S}_+(-\omega_2),$$

$$M_{13}(3,4) = -\bar{G}_+(\omega_1) - \bar{G}_+(\omega_2) + i\bar{S}_+(\omega_1) - i\bar{S}_+(\omega_2);$$

$$M_{24} = \begin{pmatrix} 0 & M_{24}(1,2) & -2\tilde{G}_-(-\omega_1) & 0 \\ M_{44}^*(1,4) & 0 & 0 & M_{24}(2,4) \\ 0 & 0 & 0 & M_{22}^*(2,3) \\ 0 & M_{13}(3,1) & M_{24}(4,3) & 0 \end{pmatrix},$$

$$M_{24}(2,4) = -\left(\tilde{G}_+(\omega_2) + \tilde{G}_+(-\omega_2) + 2\tilde{G}_+(-\omega_1)\right) - i\left(\alpha + \beta + \tilde{S}_+(\omega_2) - \tilde{S}_+(-\omega_2)\right),$$

$$M_{24}(1,2) = \bar{G}_+(-\omega_1) + \bar{G}_+(-\omega_2) + i\bar{S}_+(-\omega_1) - i\bar{S}_+(-\omega_2),$$

$$M_{24}(4,3) = -\bar{G}_-(-\omega_1) - \bar{G}_-(-\omega_2) + i\bar{S}_-(-\omega_1) - i\bar{S}_-(-\omega_2);$$

$$M_{34} = \begin{pmatrix} 0 & 2\tilde{G}_-(-\omega_2) & M_{34}(1,3) & 0 \\ 0 & 0 & 0 & M_{33}(2,3) \\ M_{44}^*(1,4) & 0 & 0 & M_{34}(3,4) \\ 0 & M_{34}(4,2) & M_{12}(2,1) & 0 \end{pmatrix},$$

$$M_{34}(3,4) = -\left(\tilde{G}_+(\omega_1) + \tilde{G}_+(-\omega_1) + 2\tilde{G}_+(-\omega_2)\right) + i\left(\alpha - \beta + \tilde{S}_+(-\omega_1) - \tilde{S}_+(\omega_1)\right),$$

$$M_{34}(1,3) = -\bar{G}_+(-\omega_1) - \bar{G}_+(-\omega_2) + i\bar{S}_+(-\omega_1) - i\bar{S}_+(-\omega_2),$$

$$M_{34}(4,2) = -\bar{G}_-(-\omega_1) - \bar{G}_-(-\omega_2) + i\bar{S}_-(-\omega_1) - i\bar{S}_-(-\omega_2);$$

$$M_{21} = M_{12}^\dagger, M_{31} = M_{13}^\dagger, M_{42} = M_{24}^\dagger, M_{43} = M_{34}^\dagger.$$

Notice that all the M_{ij} here are traceless, because $\frac{d}{dt}Tr\rho_S = \frac{d}{dt}Tr\rho_O = 0$. To obtain the steady-state solution, we set $\frac{d\rho}{dt} = 0$, that is $\frac{d\rho_S}{dt} = 0$ and $\frac{d\rho_O}{dt} = 0$. For the former, we can calculate ρ_S in a perturbative way:

$$\rho_S^{steady} = \rho_{pd}^{(0)} + \rho_{sd}^{(0)} + \lambda^2 \rho_{pd}^{(2)} + \lambda^2 \rho_{sd}^{(2)} + O(\lambda^4), \quad (B3)$$

where ρ_{pd} stands for the primary diagonal elements, ρ_{sd} stands for the secondary diagonal elements, and we know that $Tr\rho_{pd}^{(0)} = 1, Tr\rho_{pd}^{(2)} = 0$. In combination with Eq. (B1), given that both $G(\omega)$ and $S(\omega)$ are of order λ^2 , the coefficient of λ^0 in the equation gives

$$2i \begin{pmatrix} & & -\beta\rho_{14}^{(0)} \\ & -\alpha\rho_{23}^{(0)} & \\ \beta\rho_{41}^{(0)} & \alpha\rho_{32}^{(0)} & \end{pmatrix} = 0.$$

For the non-degenerate cases (the degenerate case is discussed in Appendix C), $\alpha \neq 0$, this means $\rho_{sd}^{(0)} = 0$; the coefficient of λ^2 in the diagonal gives

$$\begin{aligned} -\left(\tilde{G}_+(\omega_1) + \tilde{G}_+(\omega_2)\right)\rho_{11}^{(0)} + \tilde{G}_+(-\omega_1)\rho_{22}^{(0)} + \tilde{G}_+(-\omega_2)\rho_{33}^{(0)} &= 0, \\ \tilde{G}_+(\omega_1)\rho_{11}^{(0)} - \left(\tilde{G}_+(-\omega_1) + \tilde{G}_+(\omega_2)\right)\rho_{22}^{(0)} + \tilde{G}_+(-\omega_2)\rho_{44}^{(0)} &= 0, \\ \tilde{G}_+(\omega_2)\rho_{11}^{(0)} - \left(\tilde{G}_+(\omega_1) + \tilde{G}_+(-\omega_2)\right)\rho_{33}^{(0)} + \tilde{G}_+(-\omega_1)\rho_{44}^{(0)} &= 0, \\ \tilde{G}_+(\omega_2)\rho_{22}^{(0)} + \tilde{G}_+(\omega_1)\rho_{33}^{(0)} - \left(\tilde{G}_+(-\omega_1) + \tilde{G}_+(-\omega_2)\right)\rho_{44}^{(0)} &= 0. \end{aligned}$$

One can find that only three of these four equations are independent of each other. Considering that $Tr\rho_{pd}^{(0)} = 1$, we obtain

$$\rho_{pd}^{(0)} = \frac{1}{N} \begin{pmatrix} \tilde{G}_+(-\omega_1)\tilde{G}_+(-\omega_2) & & & \\ & \tilde{G}_+(\omega_1)\tilde{G}_+(-\omega_2) & & \\ & & \tilde{G}_+(-\omega_1)\tilde{G}_+(\omega_2) & \\ & & & \tilde{G}_+(\omega_1)\tilde{G}_+(\omega_2) \end{pmatrix},$$

with $N = (\tilde{G}_+(\omega_1) + \tilde{G}_+(-\omega_1))(\tilde{G}_+(\omega_2) + \tilde{G}_+(-\omega_2))$, which happens to coincide with the steady-state solution of the Lindblad master equation (A14)(A15). The coefficient of λ^2 in the secondary diagonal elements gives $\lambda^2\rho_{pd}^{(2)}$

$$\lambda^2\rho_{14}^{(2)} = \lambda^2\rho_{41}^{(2)*} = \frac{1}{2i\beta} \sum_{i=1}^4 M_{ii}(1,4)\rho_{ii}^{(0)}, \quad (B4)$$

$$\lambda^2\rho_{23}^{(2)} = \lambda^2\rho_{32}^{(2)*} = \frac{1}{2i\alpha} \sum_{i=1}^4 M_{ii}(2,3)\rho_{ii}^{(0)}. \quad (B5)$$

Similarly, we can obtain four equations about $\lambda^2\rho_{pd}^{(2)}$ by the coefficient of λ^4 in the primary diagonal elements, but only three of them are independent of each other, and considering $Tr\rho_{pd}^{(2)} = 0$ we can then compute $\lambda^2\rho_{pd}^{(2)}$.

As for $\frac{d\rho_O}{dt} = 0$, we find that if ρ_O is written as a column vector $|\rho_O\rangle$, then Eq. (B2) corresponds to the equation $\frac{d|\rho_O\rangle}{dt} = \mathcal{M}|\rho_O\rangle$ in which the eight-dimensional matrix \mathcal{M} is a diagonally dominant matrix:

$$|\mathcal{M}_{kk}| \sim \beta \gg \lambda^2 \sim \sum_{l \neq k} |\mathcal{M}_{kl}|,$$

so the determinant of \mathcal{M} is not zero, i.e. \mathcal{M} is invertible, thus the solution to $\mathcal{M}|\rho_O\rangle = 0$ must be a zero vector.

Appendix C: The heat current for the symmetric case as $g \rightarrow 0$

For the symmetric case, in the limit of $g \rightarrow 0$, we obtain $\varphi \rightarrow 0, \theta \rightarrow \frac{\pi}{2}, \alpha \rightarrow 0, \beta \rightarrow \varepsilon, \omega_1 = \omega_2 \rightarrow \varepsilon$. Substituting these into Eq. (24), we get

$$\mathcal{J}^L = \frac{J(\varepsilon)(\bar{n}_1(\varepsilon) - \bar{n}_2(\varepsilon))}{1 + \bar{n}_1(\varepsilon) + \bar{n}_2(\varepsilon)} (\varepsilon + \delta) \quad (C1)$$

with $\delta = (S_1(\varepsilon) + S_2(\varepsilon) - S_1(-\varepsilon) - S_2(-\varepsilon))/2$, where we have taken $\gamma_1 = \gamma_2$ for simplicity, so that $J_1(\varepsilon) = J_2(\varepsilon) \equiv J(\varepsilon)$. \mathcal{J}^L is a non-zero value at $T_1 \neq T_2$, which is unphysical. In the limit $g \rightarrow 0$, the system decouples into two independent subsystems, effectively eliminating any interaction between the thermal reservoirs. Consequently, the heat current must vanish to maintain consistency with thermodynamic principles.

But in the BR master equation, substituting these into M_{ij} , the exact steady-state solution can be achieved by the non-perturbative direct solution method as

$$\rho_S = \frac{1}{(1+2n_1)(1+2n_2)} \begin{pmatrix} n_1 n_2 & & & \\ & n_1 n_2 + \frac{n_1+n_2}{2} & \frac{n_2-n_1}{2} & \\ & & n_1 n_2 + \frac{n_1+n_2}{2} & \\ & & & (n_1+1)(n_2+1) \end{pmatrix},$$

where $n_1 = \bar{n}_1(\varepsilon)$, $n_2 = \bar{n}_2(\varepsilon)$, it can be seen that this steady-state solution coincides with a unitary transformation of the direct product of the local thermal state of the two TLAs, which implies the steady-state solution of the local master equation. From Eq. (22), it can be calculated that the heat current is zero, which is in agreement with the previous discussion. This shows that in our model, the BR master equation degenerates into the local Lindblad master equation only in the symmetric case, and if the internal coupling of the system is very weak, for $\varepsilon_1 \neq \varepsilon_2$ the BR master equation does not degenerate into the local Lindblad master equation even though the internal coupling of the system is very weak.

This explains why the heat current predicted by the local Lindblad master equation at $\varepsilon_1 \neq \varepsilon_2$ sometimes violates the second law of thermodynamics [73, 74], since the BR master equation in this case does not approximate the local Lindblad master equation. This is consistent with the results obtained by a recently developed master equation based on subsystem eigenstates [39], which provides a second-order approximation to the BR master equation as g tends to zero.
